Check for updates

Laser & Photonics Reviews

LASER & PHOTONICS REVIEWS

www.lpr-journal.org

RESEARCH ARTICLE

The Magnetic Dislocation for Trapping and Adiabatic Conversion of Light

Danying Yu[1] | Kun Ding[2] | Xianfeng Chen[1,3,4] | Luqi Yuan[1]

[1]State Key Laboratory of Photonics and Communications, School of Physics and Astronomy, Shanghai Jiao Tong University, Shanghai, China | [2]Department of Physics, State Key Laboratory of Surface Physics, and Key Laboratory of Micro and Nano Photonic Structures (Ministry of Education), Fudan University, Shanghai, China | [3]Shanghai Research Center for Quantum Sciences, Shanghai, China | [4]Collaborative Innovation Center of Light Manipulations and Applications, Shandong Normal University, Jinan, China

Correspondence: Kun Ding (kunding@fudan.edu.cn) | Luqi Yuan (yuanluqi@sjtu.edu.cn)

Received: 15 November 2024 | **Revised:** 7 October 2025 | **Accepted:** 11 October 2025

Keywords: adiabatically pumping | light manipulation | magnetic dislocation | topological defect

ABSTRACT

The dislocation created in the topological material lays the foundation of many significant findings to control light but requires delicate fabrication of the material. To extend its flexibility and reconfigurability, we propose the magnetic dislocation concept and unveil its properties in a representative model, which effectively combines the topological defect and edge mode at the magnetic domain wall. The results include distinct localization modes and robust light trapping phenomena with the rainbow feature where the eigen-energy of each light-trapping state can be linearly tuned by the magnetic dislocation. The conversion from the trapping state to edge modes can be harnessed by further adiabatically pumping light across an amount of the magnetic dislocation variation. Our work solves a fundamental problem involving reconfigurability by introducing magnetic dislocation with new light-manipulation flexibility, which may be implemented in a variety of platforms in photonic, acoustics, and optomechanics with dynamic modulations and synthetic dimensions.

1 | Introduction

Dislocation, as the topological defect, describes the distortion of the hosting lattice, usually characterized as the real-space topology that cannot be eliminated by local continuous modifications [1–4]. Recently, it has been realized that the interplay between dislocations and band topology in topological materials brings novel ways in light manipulations against disorders [5–21], including the light-trapping [13], bulk probes of higher-order topological insulators [18], simulating 3D topology [20, 22–24], controlling the topology of material [21], and probing the topology of the system [25, 26]. Besides, the dislocation has its unique functionality for the study of topological insulators, especially for the realization of strong photonics topological insulators in 3D space [27]. The defect associated with dislocation is known as the topological defect due to the concomitant magnetic vortex brought by the spatial variation [11, 13]. Previous studies have focused on the dislocation configurations from spatially designed topological defect [4, 5, 13, 21, 28–31], which has limited reconfigurability, particularly in the optical regime [32].

The effective magnetic field for photonics provides a powerful approach to control the motion of light in a flexible way [33–39], with which the photonic analogy of quantum Hall effect can be realized in photonics platforms [34–37]. As for dislocation in the hosting lattice, it has been indicated that the effective gauge potential generated from the geometrical dislocation is the main reason affecting the property of the topological defect mode [4]. It is, therefore, of fundamental interest to explore the direct dislocation in an effective magnetic field, namely *magnetic dislocation*, in photonics, which not only deepens the fundamental understanding of the dislocation mechanism but also shows new potential in reconfigurable light manipulation.

© 2025 Wiley-VCH GmbH

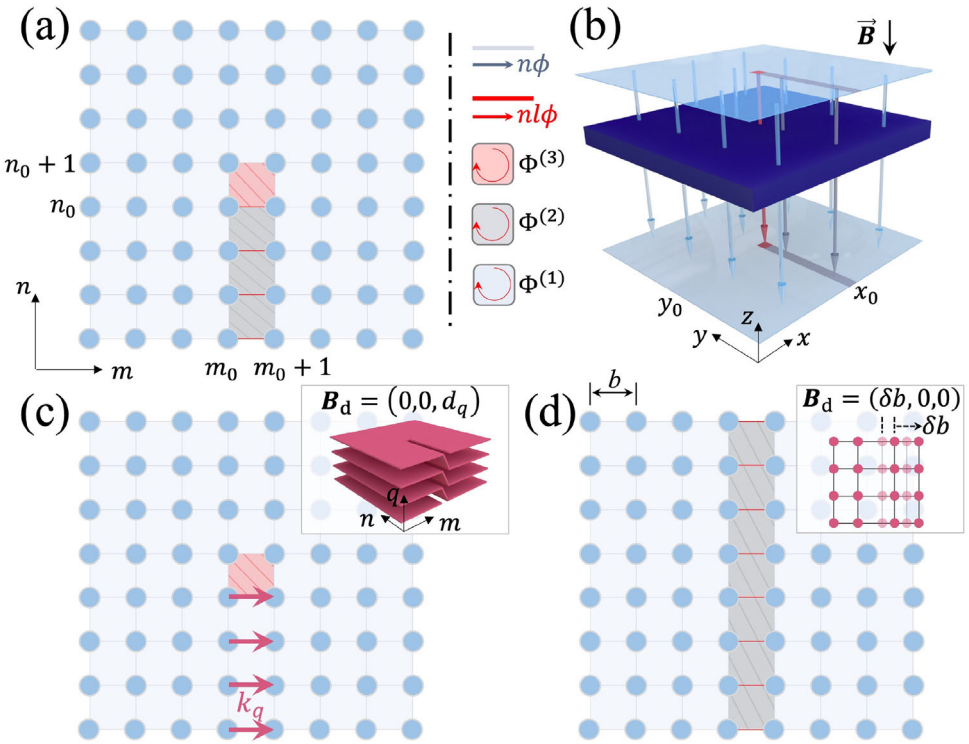

FIGURE 1 | The model of the magnetic dislocation. a) The 2D lattice with the designed distribution of hopping phases. b) The continuous model subjected to a non-uniform magnetic field (see Supporting Information). c) The deformation along the q dimension forms a 3D screw dislocation, which can be effectively characterized by deforming the magnetic field at the center (the magnetic singularity). d) The deformation along the m dimension forms the glide of the lattice sites, which can be effectively characterized by deforming the magnetic field in the middle (domain wall). Zoom-in figures label the corresponding Burger vectors to characterize deformations in (c) and (d).

In this work, we theoretically study the fundamental problem of the magnetic dislocation in a spatially uniform tight-binding (TB) lattice. The magnetic dislocation is introduced by designing non-continuously distributed hopping phases to construct a magnetic singularity in the underlying lattice without spatial defect, as shown in Figure 1a. The introduction of such artificial magnetic dislocation is in-principle different from previous models with dislocation well-defined in spatial structures [4, 40], but is universal to be possibly constructed for waves using recent experimental technologies in photonics [41–43], acoustics [44, 45], and optomechanics [46–48]. We unveil such concept of magnetic dislocation as the composition of two effective mechanisms, namely the topological defect and edge mode at the magnetic domain wall simultaneously. Therefore, by tuning the discontinuous hopping phase, light can be trapped at the singularity of the magnetic flux with the rainbow feature [49, 50], i.e., the eigen-energy of each light-trapping state varies with the tuning of the magnetic dislocation monotonically. Such light trapping state can be converted to edge modes by adiatically pumping the light. Our proposal can be generalized to all electromagnetic waves [51], which may trigger further research interest in topological defects with magnetic singularities and novel wave manipulations [52–54].

2 | Model

We consider a 2D topological lattice model including a uniform effective magnetic flux (see Figure 1). The Landau gauge is taken with horizontal hopping phases on the n-th row as $n\phi$ [55], which supports a uniform effective magnetic field $B_{\text{eff}} = \frac{1}{b^2}\int_{\text{plaquette}} A_{\text{eff}} dr = \frac{\phi}{b^2}$ [34], with A_{eff} being the effective gauge potential and b being the lattice constant. We take $\phi = \pi/2$ throughout this paper. The corresponding Hamiltonian is

$$H = \sum_{m,n} \kappa a^{\dagger}_{m,n} a_{m+1,n} e^{-in\phi} + \kappa a^{\dagger}_{m,n} a_{m,n+1} + h.c., \tag{1}$$

where $a^{\dagger}_{m,n}(a_{m,n})$ is the creation (annihilation) operator and κ is the coupling strength. Like the quantum Hall effect in the electronic system, the effective magnetic field imposed on photons makes the system topologically non-trivial with edge states [36].

On the basis of this conventional model (1), we introduce the dislocation directly in the magnetic field. As illustrated in Figure 1a, we modify hopping phases between m_0-th and (m_0+1)-th columns from $n\phi$ to $nl\phi$ for those horizontal hoppings at $n \le n_0$, where n_0 labels a fixed position, and the real number l is a parameter that brings the discontinuity and determines the magnitude of the magnetic dislocation (while the magnetic field is uniform if $l = 1$). The designed magnetic dislocation refers to the counterpart of edge dislocation in spatial geometry [13, 14, 18, 25, 56, 57], which gives three types of magnetic fluxes inside the lattice, the one in the middle plaquette in Figure 1a is $\Phi^{(3)} = (n_0+1)\phi - n_0 l\phi$, fluxes in each plaquette underneath is $\Phi^{(2)} = l\phi$, and all rest gives $\Phi^{(1)} = \phi$. The introduced magnetic dislocation could be linked to the continuous model with the magnetic field supporting the magnetic singularity in the middle

18638899, 2026, 6, Downloaded from https://onlinelibrary.wiley.com/doi/10.1002/lpor.202401951 by Shanghai Jiaotong University, Wiley Online Library on [11/05/2026]. See the Terms and Conditions (https://onlinelibrary.wiley.com/terms-and-conditions) on Wiley Online Library for rules of use; OA articles are governed by the applicable Creative Commons License

and corresponding line discontinuity (see Figure 1b with details in Supporting Information).

The discontinuous distribution of hopping phase can promisingly be fulfilled in photonics with tailored designs [58], for example, a synthetic frequency lattice built in coupled ring systems under dynamic modulations that supports hopping phase $n\phi$ along the frequency axis of light [36, 43, 59–65]. By adding auxiliary ring to split resonant frequency mode and then modulating the frequency between split supermodes with designed modulation phase, one can construct the effective hopping phase $nl\phi$. Therefore, in this photonics platform, the parameter l can be tuned by varying the amplitude of the modulation phase between split supermodes (see Supporting Information for details). Besides, other implementations involving acoustics [66] and optomechanics [47] with the supporting of effective gauge field [34, 35, 42, 67] can possibly fulfill the magnetic dislocation.

In contrast to the dislocation from distortion of the hosting lattice [27], our model of magnetic dislocation does not vary the lattices, but the underlying mechanism can be interpreted in terms of the real space dislocation as the composition of two effective mechanisms with different Burger vectors, i.e., the singularity of the flux $\Phi^{(3)}$ is equivalent to the topological-defect model in Figure 1c while the line discontinuity of the flux $\Phi^{(2)}$ corresponds to a magnetic domain wall described in Figure 1d. The former model gives the topological defect as $-\Phi^{(3)}+\phi$ in 2D plane, which can be mapped to an effective momentum k_q along the third dimension q. The screw dislocation is thus formed in a 3D lattice with the Burger vector being $B_{\rm d}=(0,0,d_q)$, where d_q is the lattice constant along the q dimension. The latter one supports edge modes from breaking time-reversal symmetry at the middle magnetic domain wall, which supports $B_{\rm d}=(\delta b,0,0)$, with $\delta b=(l-1)b$ from the magnetic deformation (see Supporting Information for details). Note that the magnetic dislocation in Figure 1a only supports half of the effective domain-wall model in Figure 1d.

3 | Results

The Hamiltonian describing the lattice with the magnetic dislocation in Figure 1a reads,

$$H_d=\sum_{\substack{m=m_0,\\ n\le n_0}}(\kappa a^{\dagger}_{m,n}a_{m+1,n}e^{-inl\phi}+\kappa a^{\dagger}_{m,n}a_{m,n+1}+h.c.)+\sum_{\text{others}}(\kappa a^{\dagger}_{m,n}a_{m+1,n}e^{-in\phi}+\kappa a^{\dagger}_{m,n}a_{m,n+1}+h.c.). \quad (2)$$

The intrinsic feature of the lattice structure can be uncovered by analyzing the spectra and the eigen-state distribution under the periodic boundary condition (PBC), where the parameters are set as $m\in[1,40]$, $n\in[1,40]$, $m_0=20$, $n_0=20$. We first select $l=0.15$ to showcase different features from the magnetic dislocation.

In the plotted spectrum in Figure 2a, the immediate observation lies on the existence of multiple eigen-modes inside bulk gaps open by the background flux $\Phi^{(1)}$. We choose one mode at $E=1.4\kappa$ and plot the eigen-state distribution in Figure 2b, which shows the localization feature at lattice sites (m,n) with $m=20$ or 21 and $n\le n_0$. Such eigen-state distribution is from the line discontinuity from the magnetic dislocation, dubbed as *line localization mode*.

In Figure 2c, we take $E=2.39\kappa$, and plot the eigen-state distribution. One notes that it exhibits strong localization near the magnetic singularity (20,20) that gives *point localization mode*. Interestingly, these localization effects hold stable when the lattice size is increasing (see Supporting Information). As a side note, the PBC we take here can induce the artificial discontinuity of the hopping phases along columns at $n=1$ and $n=40$. The eigen-state distribution in Figure 2b extends to the vicinity of top two middle sites. Such extension disappears once we consider a finite lattice model with open boundary condition (OBC) in following simulations.

To quantitatively distinguish bulk modes and localization modes in the spectrum, we define the criterion using the inverse participation ratio (IPR) to characterize the mode feature, i.e., $\text{IPR}\equiv\left[\sum_{m,n}|\psi_{m,n}|^4\right]/\left[\sum_{m,n}|\psi_{m,n}|^2\right]^2$ with $\psi_{m,n}$ being the eigen-state amplitude. A standard point localization mode shown in Figure 2e has IPR = 0.25, refer the localization in the vicinity of the position of the singularity. For a standard line localization mode in Figure 2d, IPR = 0.025 as the distribution in the lower half part extends among $n\in[1,20]$ in the middle of the m-axis. As for a typical bulk mode with distribution equally spread out the whole lattice, $\text{IPR}=6.25\times10^{-4}$.

We then explore properties of all modes in the projected spectrum versus l in Figure 3a. For $l=1$, the magnetic flux is uniformly distributed, and there is no magnetic dislocation, so no localization mode exists either. Nevertheless, for cases with $l\neq1$, the magnetic dislocation is introduced, and various types of dislocation modes appear. In particular, one sees that the line localization modes (in blue) are widely distributed outside of the bulk spectra. The most interesting feature is that the point localization modes in red monotonically increase (decrease) with the variation of l in the upper (lower) spectral gap, which gives multiple monotonic curves, and each of them shows the rainbow feature. Such rainbow distribution of point localization modes with the variation of l provides a way to selectively localize a particular frequency component of the light by varying the magnetic dislocation. Moreover, the number of these monotonic curves for the point localization modes depends on the accumulated phase at the point discontinuity (i.e., the magnetic singularity, see Supporting Information).

To demonstrate the magnetic singularity is the composition of two effective mechanisms, we perform separate spectrum analysis for both. In Figure 3b, we plot the spectrum versus k_q from the effective model described in Figure 1c, again under PBC. The bands in-between bulks refer to the topological defect with the localization feature of its eigen-state distribution (see Figure 3d). Therefore, the varying l in Figure 3a effectively equals to tuning k_q in the manner of $k_q\cdot d_q=-\Phi^{(3)}+\phi$ (with d_q being the lattice constant in the q dimension) which gives the rainbow feature of the point localization mode. The localization phenomena of the geometric defect can also be linked to the magnetic defect by uncovering the phase phase information at the defect (see Supporting Information for details). As for the magnetic domain-wall model in Figure 1d, we plot the corresponding spectrum in

18638899, 2026, 6, Downloaded from https://onlinelibrary.wiley.com/doi/10.1002/lpor.202401951 by Shanghai Jiaotong University, Wiley Online Library on [11/05/2026]. See the Terms and Conditions (https://onlinelibrary.wiley.com/terms-and-conditions) on Wiley Online Library for rules of use; OA articles are governed by the applicable Creative Commons License

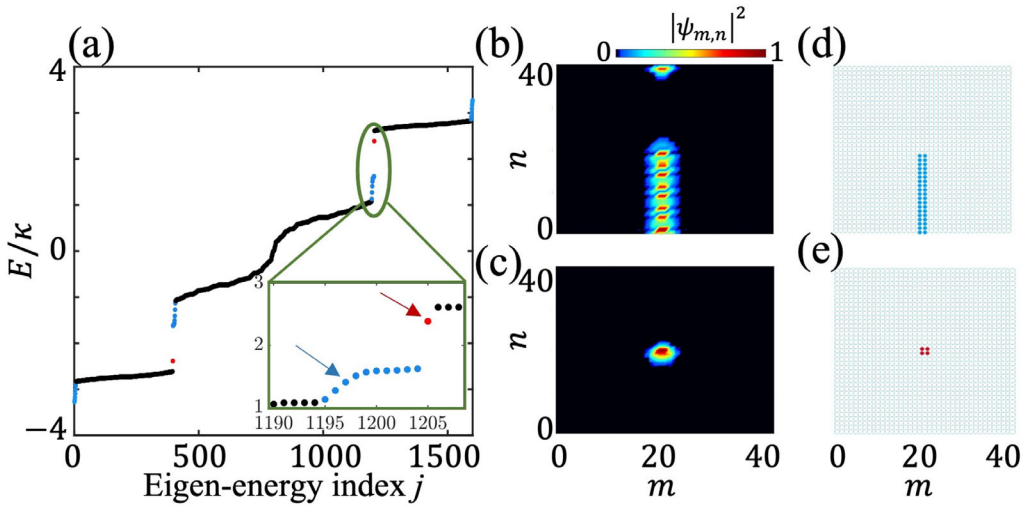

FIGURE 2 | Spectra and intensity distributions of eigen-states. a) Spectra for $l = 0.15$. Zoom-in plots are presented in green boxes. b,c) Intensity distributions of eigen-states for the eigen-energies labeled by blue and red arrows in (a). d,e) Schematic diagrams of standard line and point localization modes, respectively.

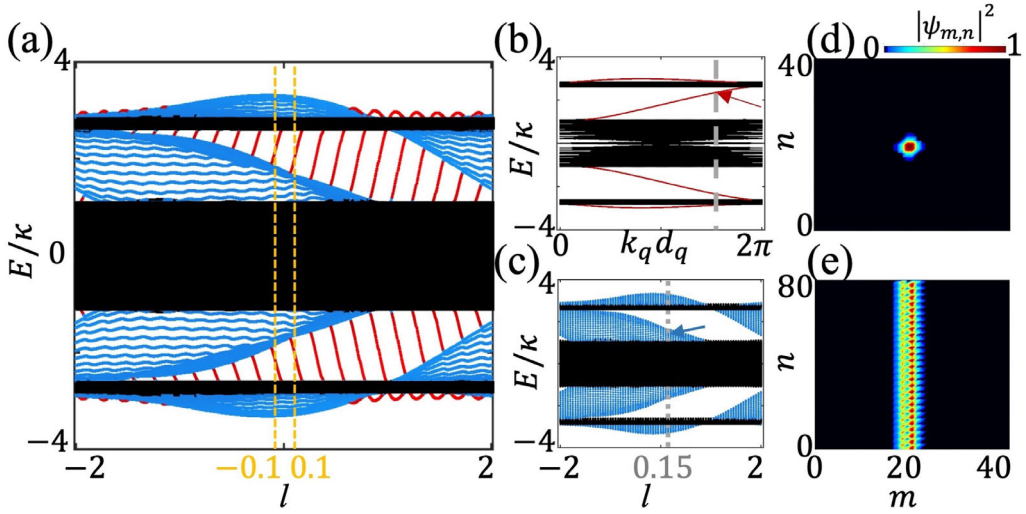

FIGURE 3 | The projected spectrum. a) The projected spectrum along parameter l, where bulk states, line localization, and point localization are characterized as IPR < 0.01 (black), $0.01 \leq$ IPR < 0.04 (blue), and IPR ≥ 0.04 (red), respectively. b,c) The spectrum from effective models in Figure 1c,d, respectively. d,e) Corresponding eigen-state distributions of two eigen-modes labeled by the red arrow in (b) and blue arrow in (c).

Figure 3c under PBC. One can see the similar spectrum with that in Figure 3a except for no point localization modes. In this effective model with the domain wall throughout the vertical range, the corresponding edge-state distribution in Figure 3e exhibits such edge mode occupying middle sites with all n.

Simulation under OBC can show the dynamic evolution of the light in a (40×40) lattice, where we choose the magnetic dislocation parameter as $l = 0.15$ in order to support point localization modes and line localization modes in-between the spectral gap. One-way edge states in-between gaps exist due to the effective magnetic flux [36]. We excite the lattice at a single lattice site with the input pulse field as $E_{\text{in}}(t) = e^{-i\omega_c t} e^{-(t-t_0)^2/\Delta t^2}$, where $t_0 = 20\kappa^{-1}$ and $\Delta t = 8\kappa^{-1}$, and study distributions of the field intensity on each site $|v_{m,n}|^2$ at different times (see Supporting Information for details). ω_c is the center frequency of the excitation.

We first excite the lattice by using $E_{\text{in}}(t)$ with $\omega_c = 2.39\kappa$ at the boundary of the lattice $(m, n) = (1, 20)$ to excite the topological one-way edge state. The simulation results are shown in Figure 4a, where three snapshots at $t = 40$, 120, and $200\kappa^{-1}$, respectively, present the evolution of the light in the lattice at different times. The edge mode is unidirectionally propagating along the boundary of the lattice without efficiently leaking into the bulk or coupling to any localization modes.

We now take the same input pulse but excite the lattice at the point discontinuity $(m, n) = (20,21)$, and show simulation results in Figure 4b. One can see that the point localization mode is successfully excited, where the light is trapped at the singularity of the magnetic dislocation, consistent with the theoretical prediction in Figure 2c. More importantly, although the input at the same excitation frequency can also excite a topological edge

18638899, 2026, 6, Downloaded from https://onlinelibrary.wiley.com/doi/10.1002/lpor.202401951 by Shanghai Jiaotong University, Wiley Online Library on [11/05/2026]. See the Terms and Conditions (https://onlinelibrary.wiley.com/terms-and-conditions) on Wiley Online Library for rules of use; OA articles are governed by the applicable Creative Commons License

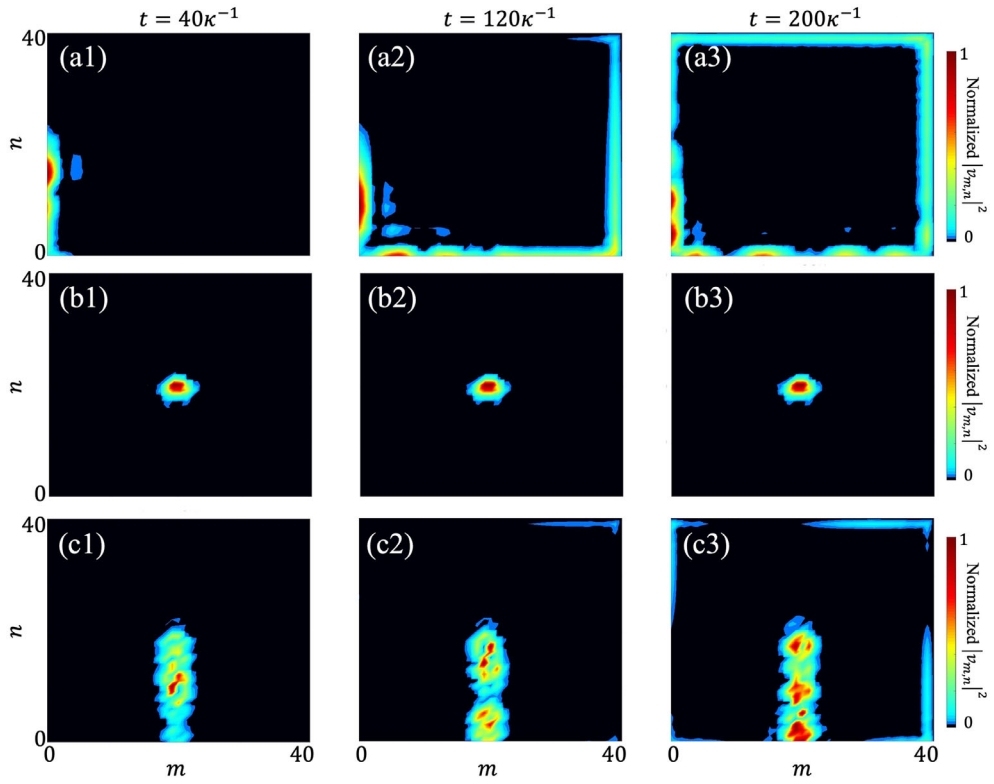

FIGURE 4 | The dynamic evolutions of the light excited by a pulse source in the finite lattice. a) Simulation results of $|v_{m,n}|^2$ at $t = 40, 120,, 200\kappa^{-1}$, respectively, with the $E_{\text{in}}(t)$ at $\omega_c = 2.39\ \kappa$ excited at $(m, n) = (1, 20)$. b) Simulation results with the same $E_{\text{in}}(t)$ at $\omega_c = 2.39\ \kappa$ but excited at $(m, n) = (20, 21)$. c) Simulation results with the same $E_{\text{in}}(t)$ but $\omega_c = 1.4\ \kappa$ excited at $(m, n) = (20,11)$.

mode if the excitation position is at the boundary of the lattice (see Figure 4a), the trapped light does not leak into the edge mode. In other words, due to the strong localization effect, the point localization mode does not interact with the edge mode due to no spatial overlap between two modes. There is no leak to the line localization mode either because of different eigen-energies for these two modes (see Figure 2a). Moreover, the excited distribution of the point localization mode is robust against possible imperfections and noises in practical experiments (see Supporting Information), so it showcases an efficient localization effect from the magnetic dislocation in photonics.

In Figure 4c, we give simulation results of exciting the lower line localization mode by using $E_{\text{in}}(t)$ with $\omega_c = 1.4\ \kappa$ at the middle of the line discontinuity $(m, n) = (20, 11)$. Here, the light is initially trapped within the line discontinuity regime, but during the time evolution, a portion of light leaks to edge modes and propagates along the boundary counter-clockwisely. Such a phenomenon indicates that even though we successfully excite the line localization mode initially, it can interact with the one-way edge mode in a finite lattice as the small overlap between two modes, and the energy of localization is then leaking out in this case. Note that the artificial extension to top sites in Figure 2b indeed disappears.

We suggest two possible applications with the unveiled light trapping with point localization modes under manipulations of the parameter l. First, we use a broadband pulse with $\Delta t = 4.62\kappa^{-1}$, $t_0 = 20\kappa^{-1}$, and $\omega_c = 1.94\ \kappa$ to excite the system at the point discontinuity $(m, n) = (20, 21)$ in various choices l. Such pulse covers a broad spectral bandwidth $\Delta\omega \sim 0.71\kappa$, spanning over the upper spectral gap in Figure 3a. We perform simulations with $l = 0.68, 0.695, 0.71, 0.725,$, and 0.74, respectively, collect field amplitudes at $(m, n) = (20, 21)$, and plot the corresponding spectra in Figure 5a. One can see the selective excitation of the localization mode with the blue shift of the frequency when l is increasing.

Next, we show the adiabatic pumping of light by exciting the system at (20, 21) with pulse parameters $\omega_c = 1.96\kappa$, $t_0 = 20\kappa^{-1}$, and $\Delta t = 8\kappa^{-1}$, and then slowly varying l from 0.1 to -0.1 shown in Figure 5b. The system is initially excited at the point localization mode and then adiabatically gets tuned into the regime of line localization modes (see Figure 3a). The simulation results show that the field is initially trapped at the middle of the lattice for $t = 40\kappa^{-1}$, $80\kappa^{-1}$, but gets converted into the line-localization distribution at $t = 120\kappa^{-1}$. Afterwards, the field slowly leaks into the edge mode. This example exhibits interesting conversion among three modes, namely point localization, line localization, and edge state modes with an adiabatic operation, showing a way for releasing the trapped light at the magnetic singularity in a controllable way.

4 | Summary

We study the magnetic dislocation in a spatially uniform lattice and explore physics of localization modes in theory. The projection of high-dimensional phase on the lower dimension gives rise to the singularity in the effective magnetic field, where

18638899, 2026, 6, Downloaded from https://onlinelibrary.wiley.com/doi/10.1002/lpor.202401951 by Shanghai Jiaotong University, Wiley Online Library on [11/05/2026]. See the Terms and Conditions (https://onlinelibrary.wiley.com/terms-and-conditions) on Wiley Online Library for rules of use; OA articles are governed by the applicable Creative Commons License

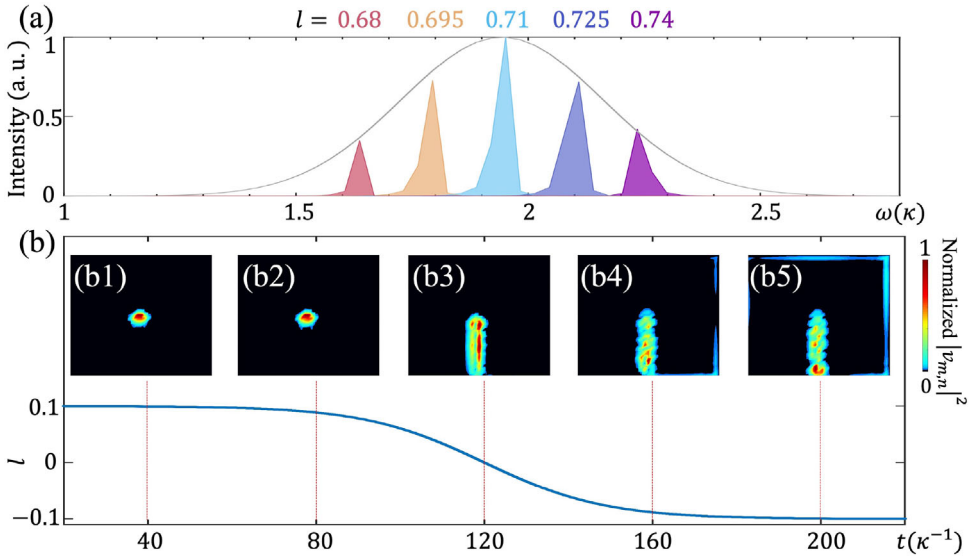

FIGURE 5 | a) The spectra of localized modes from the field collected at $(m, n) = (20, 21)$, where $l = 0.68$ (red), 0.695 (orange), 0.71 (cyan), 0.725 (blue), and 0.74 (purple) are taken in simulations. The grey curve indicates the spectrum of the input pulse. b) Adiabatic pumping of light by slowly tuning l from 0.1 to −0.1 during the time $t \in [0, 240]\kappa^{-1}$. b1–b5) Simulation results of $|v_{m,n}|^2$ at $t = 40$, 80, 120, 160, and $200\kappa^{-1}$.

light can be trapped robustly in the vicinity of the singularity without leaking into either bulk modes or edge modes. We find the rainbow featured light-trapping phenomena, which supports possible applications for fine adjustment of cavity frequency mode with tunable external modulation. Finally, the adiabatic control of the magnetic dislocation realizes the switch between trapping mode and topological edge mode. Our research explores a universal Hamiltonian in photonics, where the desired hopping phases for magnetic dislocation may be possibly realized in many experiment-feasible platforms other than the proposed synthetic frequency lattice model [68]. For example, synthetic modal space where hopping phases can be designed between propagating modes in curved waveguide arrays [42] can be another reliable candidate. For spatial photonics platforms, one can use ring arrays with designed auxiliary delayed lines for realizing desired hopping phases [35]. Moreover, the magnetic dislocation may also be generalized to other 2D symmetric lattices, for example, the C_6 symmetric lattice (see Supporting Information for more information).

Acknowledgements

The research was supported by the National Natural Science Foundation of China (12122407, 11974245, 12192252, 12174072, and 2021hwyq05), National Key Research and Development Program of China (2023YFA1407200 and 2021YFA1400900). L.Y. thanks the sponsorship from Yangyang Development Fund.

Conflicts of Interest

The authors declare no conflict of interest.

Data Availability Statement

The data that support the findings of this study are available from the corresponding author upon reasonable request.

References

1. N. D. Mermin, "The Topological Theory of Defects in Ordered Media," *Reviews of Modern Physics* 51 (1979): 591–648.

2. J. Hirth and J. Lothe, *Theory of dislocations* (McGraw Hill, 1982).

3. M. Kleman and J. Friedel, "Disclinations, Dislocations, and Continuous Defects: A Reappraisal," *Reviews of Modern Physics* 80 (2008): 61–115.

4. Z.-K. Lin, Q. Wang, Y. Liu, et al., "Topological Phenomena at Defects in Acoustic, Photonic and Solid-State Lattices," *Nature Reviews Physics* 5 (2023): 483–495.

5. Y. Ran, Y. Zhang, and A. Vishwanath, "One-Dimensional Topologically Protected Modes in Topological Insulators With Lattice Dislocations," *Nature Physics* 5 (2009): 298–303.

6. V. Juričć, A. Mesaros, R.-J. Slager, and J. Zaanen, "Universal Probes of Two-Dimensional Topological Insulators: Dislocation and π Flux," *Physical Review Letters* 108 (2012): 106403.

7. J. C. Y. Teo and T. L. Hughes, "Existence of Majorana-Fermion Bound States on Disclinations and the Classification of Topological Crystalline Superconductors in Two Dimensions," *Physical Review Letters* 111 (2013): 047006.

8. W. A. Benalcazar, J. C. Y. Teo, and T. L. Hughes, "Classification of Two-Dimensional Topological Crystalline Superconductors and Majorana Bound States at Disclinations," *Physical Review B* 89 (2014): 224503.

9. J. Paulose, B. G.-G. Chen, and V. Vitelli, "Topological Modes Bound to Dislocations in Mechanical Metamaterials," *Nature Physics* 11 (2015): 153–156.

10. H. Sumiyoshi and S. Fujimoto, "Torsional Chiral Magnetic Effect in a Weyl Semimetal With a Topological Defect," *Physical Review Letters* 116 (2016): 166601.

11. J. C. Y. Teo and T. L. Hughes, "Topological Defects in Symmetry-Protected Topological Phases," *Annual Review of Condensed Matter Physics* 8 (2017): 211–237.

12. H. Hamasaki, Y. Tokumoto, and K. Edagawa, "Dislocation Conduction in Bi-Sb Topological Insulators," *Applied Physics Letters* 110 (2017): 092105.

13. F.-F. Li, H.-X. Wang, Z. Xiong, et al., "Topological Light-Trapping on a Dislocation," *Nature Communications* 9 (2018): 2462.

14. R. Queiroz, I. C. Fulga, N. Avraham, H. Beidenkopf, and J. Cano, "Partial Lattice Defects in Higher-Order Topological Insulators," *Physical Review Letters* 123 (2019): 266802.

18638899, 2026, 6, Downloaded from https://onlinelibrary.wiley.com/doi/10.1002/lpor.202401951 by Shanghai Jiaotong University, Wiley Online Library on [11/05/2026]. See the Terms and Conditions (https://onlinelibrary.wiley.com/terms-and-conditions) on Wiley Online Library for rules of use; OA articles are governed by the applicable Creative Commons License

15. Q. Wang, H. Xue, B. Zhang, and Y. D. Chong, "Observation of Protected Photonic Edge States Induced by Real-Space Topological Lattice Defects," *Physical Review Letters* 124 (2020): 243602.

16. C. W. Peterson, T. Li, W. Jiang, T. L. Hughes, and G. Bahl, "Trapped Fractional Charges at Bulk Defects in Topological Insulators," *Nature* 589 (2021): 376–380.

17. Y. Liu, S. Leung, F.-F. Li, et al., "Bulk-Disclination Correspondence in Topological Crystalline Insulators," *Nature* 589 (2021): 381–385.

18. B. Roy and V. Juričć, "Dislocation as a Bulk Probe of Higher-Order Topological Insulators," *Physical Review Research* 3 (2021): 033107.

19. T. Nag and B. Roy, "Anomalous and Normal Dislocation Modes in Floquet Topological Insulators," *Communications Physics* 4 (2021): 157.

20. H. Xue, D. Jia, Y. Ge, et al., "Observation of Dislocation-Induced Topological Modes in a Three-Dimensional Acoustic Topological Insulator," *Physical Review Letters* 127 (2021): 214301.

21. Z.-K. Lin, Y. Wu, B. Jiang, et al., "Topological Wannier Cycles Induced by Sub-Unit-Cell Artificial Gauge Flux in a Sonic Crystal," *Nature Materials* 21 (2022): 430–437.

22. Q. Wang, Y. Ge, H.-X. Sun, et al., "Vortex States in an Acoustic Weyl Crystal With a Topological Lattice Defect," *Nature Communications* 12 (2021): 3654.

23. L. Ye, C. Qiu, M. Xiao, et al., "Topological Dislocation Modes in Three-Dimensional Acoustic Topological Insulators," *Nature Communications* 13 (2022): 508.

24. Y. Qi, H. He, and M. Xiao, "Manipulation of Acoustic Vortex With Topological Dislocation States," *Applied Physics Letters* 120 (2022): 212202.

25. A. Panigrahi, R. Moessner, and B. Roy, "Non-Hermitian Dislocation Modes: Stability and Melting Across Exceptional Points," *Physical Review B* 106 (2022): L041302.

26. Y. Wu, Z.-K. Lin, Y. Yang, Z. Song, F. Li, and J.-H. Jiang, "Probing Fragile Topology With a Screw Dislocation," *Science Bulletin* 69 (2024): 3657–3660.

27. E. Lustig, L. J. Maczewsky, J. Beck, et al., "Photonic Topological Insulator Induced by a Dislocation in Three Dimensions," *Nature* 609 (2022): 931–935.

28. E. D. Epstein, L. Singh, M. Fox, S. Sternklar, and Y. Gorodetski, "Topological Dislocations for Plasmonic Mode Localization in Arrays of Nanoscale Rectangular Au Apertures: Implications for Optical Communications," *ACS Applied Nano Materials* 4 (2021): 1202–1208.

29. J. A. Iglesias Martínez, N. Laforge, M. Kadic, and V. Laude, "Topological Waves Guided by a Glide-Reflection Symmetric Crystal Interface," *Physical Review B* 106 (2022): 064304.

30. V. Laude, J. A. I. Martínez, N. Laforge, M. Kadic, and E. Prodan, "Glide-Reflection Symmetric Phononic Crystal Interface: Variation on a Theme," *Acta Mechanica Sinica* 39 (2023): 723016.

31. Y. Zhang, N. Manjunath, G. Nambiar, and M. Barkeshli, "Quantized Charge Polarization as a Many-Body Invariant in $(2+1)$D Crystalline Topological States and Hofstadter Butterflies," *Physical Review X* 13 (2023): 031005.

32. X.-D. Chen, F.-L. Shi, J.-W. Liu, et al., "Second Chern Crystals With Inherently Non-Trivial Topology," *Natural Science Review* 10 (2023): nwac289.

33. M. Hafezi, E. A. Demler, M. D. Lukin, and J. M. Taylor, "Robust Optical Delay Lines With Topological Protection," *Nature Physics* 7 (2011): 907–912.

34. K. Fang, Z. Yu, and S. Fan, "Realizing Effective Magnetic Field for Photons by Controlling the Phase of Dynamic Modulation," *Nature Photonics* 6 (2012): 782–787.

35. M. Hafezi, S. Mittal, J. Fan, A. Migdall, and J. M. Taylor, "Imaging Topological Edge States in Silicon Photonics," *Nature Photonics* 7 (2013): 1001–1005.

36. L. Yuan, Y. Shi, and S. Fan, "Photonic Gauge Potential in a System With a Synthetic Frequency Dimension," *Optics Letters* 41 (2016): 741–744.

37. T. Ozawa, H. M. Price, N. Goldman, O. Zilberberg, and I. Carusotto, "Synthetic Dimensions in Integrated Photonics: From Optical Isolation to Four-Dimensional Quantum Hall Physics," *Physical Review A* 93 (2016): 043827.

38. M. M. Denner and F. Schindler, "Magnetic Flux Response of Non-Hermitian Topological Phases," *SciPost Physics* 14 (2023): 107.

39. D. Yu, G. Li, L. Wang, D. Leykam, L. Yuan, and X. Chen, "Moiré Lattice in One-Dimensional Synthetic Frequency Dimension," *Physical Review Letters* 130 (2023): 143801.

40. S. S. Yamada, T. Li, M. Lin, C. W. Peterson, T. L. Hughes, and G. Bahl, "Bound States at Partial Dislocation Defects in Multipole Higher-Order Topological Insulators," *Nature Communications* 13 (2022): 2035.

41. A. Regensburger, C. Bersch, M.-A. Miri, G. Onishchukov, D. N. Christodoulides, and U. Peschel, "Parity-Time Synthetic Photonic Lattices," *Nature* 488 (2012): 167–171.

42. E. Lustig, S. Weimann, Y. Plotnik, et al., "Photonic Topological Insulator in Synthetic Dimensions," *Nature* 567 (2019): 356–360.

43. A. Dutt, Q. Lin, L. Yuan, M. Minkov, M. Xiao, and S. Fan, "A Single Photonic Cavity With two Independent Physical Synthetic Dimensions," *Science* 367 (2020): 59–64.

44. Z. Yang, F. Gao, X. Shi, et al., "Topological Acoustics," *Physical Review Letters* 114 (2015): 114301.

45. Y.-G. Peng, C.-Z. Qin, D.-G. Zhao, et al., "Experimental Demonstration of Anomalous Floquet Topological Insulator for Sound," *Nature Communications* 7 (2016): 13368.

46. S. Manipatruni, J. T. Robinson, and M. Lipson, "Optical Nonreciprocity in Optomechanical Structures," *Physical Review Letters* 102 (2009): 213903.

47. F. Ruesink, M.-A. Miri, A. Alù, and E. Verhagen, "Nonreciprocity and Magnetic-Free Isolation Based on Optomechanical Interactions," *Nature Communications* 7 (2016): 13662.

48. K. Fang, J. Luo, A. Metelmann, et al., "Generalized Non-Reciprocity in an Optomechanical Circuit via Synthetic Magnetism and Reservoir Engineering," *Nature Physics* 13 (2017): 465–471.

49. C. Lu, C. Wang, M. Xiao, Z. Q. Zhang, and C. T. Chan, "Topological Rainbow Concentrator Based on Synthetic Dimension," *Physical Review Letters* 126 (2021): 113902.

50. C. Lu, Y.-Z. Sun, C. Wang, et al., "On-Chip Nanophotonic Topological Rainbow," *Nature Communications* 13 (2022): 2586.

51. L. Lang, G. Yingchi, Z. Zhichao, et al., "Photon Total Angular Momentum Manipulation," *Advanced Photonics* 5 (2023): 056002.

52. W. Liu and A. E. Miroshnichenko, "Beam Steering With Dielectric Metalattices," *ACS Photonics* 5 (2018): 1733–1741.

53. I. Krešić, K. G. Makris, and S. Rotter, "Light Confinement by Local Index Tailoring in Inhomogeneous Dielectrics," *Laser & Photonics Reviews* 15 (2021): 2100115.

54. W. Wang, X. Wang, and G. Ma, "Extended State in a Localized Continuum," *Physical Review Letters* 129 (2022): 264301.

55. D. R. Hofstadter, "Energy Levels and Wave Functions of Bloch Electrons in Rational and Irrational Magnetic Fields," *Physical Review B* 14 (1976): 2239–2249.

56. B. A. Bhargava, I. C. Fulga, J. van den Brink, and A. G. Moghaddam, "Non-Hermitian Skin Effect of Dislocations and its Topological Origin," *Physical Review B* 104 (2021): L241402.

57. S. K. Das and B. Roy, "Dynamic Melting and Condensation of Topological Dislocation Modes," *Physical Review B* 108 (2023): 144304.

58. Z. Chen and M. Segev, "Highlighting Photonics: Looking Into the Next Decade," *Elight* 1 (2021): 2.

18638899, 2026, 6, Downloaded from https://onlinelibrary.wiley.com/doi/10.1002/lpor.202401951 by Shanghai Jiaotong University, Wiley Online Library on [11/05/2026]. See the Terms and Conditions (https://onlinelibrary.wiley.com/terms-and-conditions) on Wiley Online Library for rules of use; OA articles are governed by the applicable Creative Commons License

59. K. Wang, A. Dutt, C. C. Wojcik, and S. Fan, "Topological Complex-Energy Braiding of Non-Hermitian Bands," *Nature* 598 (2021): 59–64.

60. A. Dutt, L. Yuan, K. Y. Yang, et al., "Creating Boundaries Along a Synthetic Frequency Dimension," *Nature Communications* 13 (2022): 3377.

61. G. Li, L. Wang, R. Ye, et al., "Observation of Flat-Band and Band Transition in the Synthetic Space," *Advanced Photonics* 4 (2022): 036002.

62. A. Senanian, L. G. Wright, P. F. Wade, H. K. Doyle, and P. L. McMahon, "Programmable Large-Scale Simulation of Bosonic Transport in Optical Synthetic Frequency Lattices," *Nature Physics* 19 (2023): 1333–1339.

63. D. Cheng, E. Lustig, K. Wang, and S. Fan, "Multi-Dimensional Band Structure Spectroscopy in the Synthetic Frequency Dimension," *Light: Science & Applications* 12 (2023): 158.

64. G. Li, L. Wang, R. Ye, et al., "Direct Extraction of Topological Zak Phase With the Synthetic Dimension," *Light: Science & Applications* 12 (2023): 81.

65. F. Pellerin, R. Houvenaghel, W. A. Coish, I. Carusotto, and P. St-Jean, "Wave-Function Tomography of Topological Dimer Chains with Long-Range Couplings," *Physical Review Letters* 132 (2024): 183802.

66. H. Xue, Y. Yang, and B. Zhang, "Topological Acoustics," *Nature Reviews Materials* 7 (2022): 974–990.

67. M. C. Rechtsman, J. M. Zeuner, Y. Plotnik, et al., "Photonic Floquet Topological Insulators," *Nature* 496 (2013): 196–200.

68. D. Yu, W. Song, L. Wang, et al., "Comprehensive Review on Developments of Synthetic Dimensions," *Photonics Insights* 4 (2025): R06.

Supporting Information

Additional supporting information can be found online in the Supporting Information section.

Supporting File: lpor70555-sup-0001-SuppMat.pdf.

18638899, 2026, 6, Downloaded from https://onlinelibrary.wiley.com/doi/10.1002/lpor.202401951 by Shanghai Jiaotong University, Wiley Online Library on [11/05/2026]. See the Terms and Conditions (https://onlinelibrary.wiley.com/terms-and-conditions) on Wiley Online Library for rules of use; OA articles are governed by the applicable Creative Commons License